

Low Weight Fermionic Encodings for Lattice Models

Charles Derby^{1,2} and Joel Klassen ^{*1}

¹Phasecraft Ltd.

²Department of Computer Science, University College London

March 17, 2020

Abstract

We present two fermion to qubit encodings tailored to square and hexagonal lattices that preserve the locality of even fermionic operators. These encodings use fewer than 1.5 qubits per fermionic mode, and the generators of the even fermionic algebra have maximum Pauli weight 3. When applied to the Fermi-Hubbard model this encoding results in hopping and onsite terms with at most Pauli weight 3. As far as we are aware no other local fermionic encoding has as small a qubit to mode ratio, or as low an upper bound on the Pauli weights of the terms in the Fermi-Hubbard model.

1 Introduction

Fermion to qubit encodings are an essential ingredient in the simulation of fermionic systems on quantum devices. The earliest encodings [WJ28; BK02] map systems of M fermionic modes to M qubits; however in these encodings local fermionic interactions are mapped to non-local operators whose support scales with system size. Indeed it is effectively argued in [LW03] that without increasing the number of qubits and encoding the fermions in a subspace, non-local operators are unavoidable. To resolve this issue a number of encodings have been developed with the general goal of preserving the geometric locality of operators [BK02; VC05; WHT16; Jia+18; SW19; Set+19]. Much of the focus of recent work has been to construct encodings of this type for specific hardware layouts, for general graphs, to improve the code distance, or else to minimize qubit number.

The primary near term challenge for quantum computing devices is decoherence and the lack of quantum error correction, which severely limits run-times of quantum algorithms. This is in contrast to qubit numbers, which have been steadily rising. One of the factors that affect the run-time of a fermionic quantum simulation is the Pauli weights of the Hamiltonian terms. This is particularly true for near term analogue quantum simulation schemes, as pointed out in [HTW17]. For similar reasons, lowering the weights of terms in fermionic

*Please direct correspondence to joel@phasecraft.io

Hamiltonians is also likely to improve the performance of other quantum algorithms, such as VQE [Cad+19]. As such it may be prudent to design fermion to qubit encodings which minimize the Pauli weight of terms in the fermionic systems being simulated, even potentially at the expense of qubit number, generality or planarity of interaction graph, or code distance. One of the more likely fermionic systems to be simulated on near term devices is the Fermi-Hubbard model on a regular lattice. Here we present two fermion to qubit encodings designed for square and hexagonal lattices, which aim to minimize the Pauli weight of terms in simple fermionic lattice models such as the Fermi-Hubbard model. For these encodings, the Pauli weight of the Fermi-Hubbard terms is at most 3, and what is more, the qubit to mode ratio is at most 1.5.

2 Prior Work

All encodings which preserve the locality of fermionic operators only do so for the even fermionic operators. They do this by encoding the fermionic Fock space into a stabilized subspace of a larger multi-qubit Hilbert space.

These codes use one of two approaches. The codes in [VC05; WHT16; SW19] define stabilizers that cancel out parts of non-local qubit representations in the Jordan-Wigner encoding without affecting the simulated physics. The codes in [BK02; Set+19; Jia+18] restrict to the even fermion number subspace and construct operators that reproduce the properties of the corresponding subalgebra’s generators. Stabilizers are assigned to ensure that certain cycle operators act as identity on the code space.

Table 1 shows the performance of these codes when simulating the Fermi Hubbard model as well as some other general properties.

3 Summary of Results

In this work we present two fermion to qubit encodings designed for square and hexagonal lattices. The aim of these encodings is to minimize the Pauli weights of terms in the Fermi-Hubbard model. The encodings follow a similar logic to the encodings in [BK02; Set+19; Jia+18]. More specifically each encoding is a stabilizer code. This code is constructed by first specifying the generators of the even fermionic algebra, which consist of edge and vertex operators that anti-commute when overlapping and commute otherwise. The stabilizers of the code are then all cycles of edge operators.

The square and hexagonal encodings lead to Fermi-Hubbard terms which are at most Pauli weight 3. The number of qubits in these encodings are less than 1.5 times the number of fermionic modes. A summary is given in Table 2. As far as we know (see Table 1) no other fermionic encodings have such a small upper

¹This encoding is tailored to hardware with a particular connectivity and incorporates spin degrees of freedom into the hardware layout. This is not a constraint imposed on any of the other encodings, nor our encoding. So this is likely not an entirely fair comparison.

Reference	[BK02]	[VC05; WHT16]	[Jia+18]	[SW19] ¹	[Set+19]
Qubit Number	$4L(L-1)$	$4L^2$	$4L(L-1)$	$4L^2 - 2L$	$6L^2$
Qubit to Mode Ratio	$2 - \frac{2}{L}$	2	$2 - \frac{2}{L}$	$2 - \frac{1}{L}$	3
Max Weight Hopping	6	4	4	5	4
Max Weight Coulomb	8	2	6	6	6
Encoded Fermionic Space	Even	Full	Even	Full	Even
Graph Types	General	General	Square Lattice	Square Lattice	General
Corrects Single Qubit Errors?	No	No	Yes	No	Yes

Table 1: The qubit number and max Pauli weights of the geometrically local fermionic encodings when encoding the Fermi-Hubbard model on an $L \times L$ grid ($2L^2$ modes). Also included are their supported interaction graphs as well as error correcting ability.

bound on the Pauli weight of the Fermi-Hubbard terms, or for that matter on the generators of the even fermionic algebra. Furthermore no other local fermionic encodings employ as few qubits per mode. It should be noted that these codes neither correct nor detect every single qubit error. Furthermore these codes do not consider any particular interaction geometry of the hardware.

The square and hexagonal encodings are built from a general scheme. Every edge is given an orientation. A uniform ansatz is chosen for all edge operators, given by a Pauli X on the tail end of the edge and a Pauli Y on the head. Then additional qubits are added on faces to ensure the correct anti-commutation relations when arrows do not touch head to tail. Finally, the vertex operators are Z , which is guaranteed to anti-commute with all edge operators by construction. Despite having been employed in this case for square and hexagonal lattices, this general scheme may in principle be generalized to other graphs.

4 The Even Fermionic Algebra

Fermionic systems exist in a Fock space $F = F^E \oplus F^O$ where F^E and F^O are subspaces of states with even and odd particle number respectively, dubbed the even and odd fermionic subspaces. Most natural fermionic Hamiltonians are sums of products of even fermionic operators $a_k^\dagger a_k$, $a_j^\dagger a_k$, $a_j a_k$ and $a_j^\dagger a_k^\dagger$ which preserve even/odd subspaces. Here a_k^\dagger and a_k are the standard fermionic creation and annihilation operators. The algebra of such even fermionic opera-

Lattice Type	$L \times L$ Square w/ even face number	$L \times L$ Square w/ majority even faces	$L \times L$ square w/ majority odd faces	hexagonal face centered $L \times L$ square shape
Fermionic modes	$2L^2$	$2L^2$	$2L^2$	$2(2L^2 + 4L)$
Qubit Number	$3L^2 - L$	$3L^2 - L - 1$	$3L^2 - L + 1$	$2(3L^2 + 4L)$
Qubit to Mode Ratio	$1.5 - \frac{2}{L}$	$1.5 - \frac{2}{L} - \frac{1}{2L^2}$	$1.5 - \frac{2}{L} + \frac{1}{2L^2}$	$1.5 - \frac{1}{L+2}$
Max Weight Hopping	3	3	3	3
Max Weight Coulomb	2	2	2	2
Encoded Fermionic Space	Full	Even	Full Plus Qubit	Full
Corrects Single Qubit Errors?	No	No	No	No

Table 2: The qubit number and max Pauli weights, for the Fermi-Hubbard model, of the fermionic encodings presented in this work.

tors can be generated by the edge operators E_{jk} and vertex operators V_j which satisfy the following relations [BK02]:

$$V_j^\dagger = V_j, \quad E_{jk}^\dagger = E_{jk}, \quad V_j^2 = 1, \quad E_{jk}^2 = 1, \quad E_{jk} = -E_{kj}, \quad (1)$$

$$i \neq j \neq k \neq m \neq n : [V_j, V_k] = 0, \quad [E_{ij}, V_k] = 0, \quad [E_{ij}, E_{mn}] = 0, \quad (2)$$

$$\{E_{jk}, V_j\} = 0, \quad \{E_{ij}, E_{jk}\} = 0, \quad (3)$$

A cycle $p = \{p_1, p_2, \dots\}$ is a sequence of fermionic sites such that (p_i, p_{i+1}) is an edge of the lattice, and $p_1 = p_{|p|}$.

$$\forall \text{ cycles } p : i^{(|p|-1)} \prod_{i=1}^{(|p|-1)} E_{p_i p_{i+1}} = 1. \quad (4)$$

The above relations can be most readily checked by employing the Majorana algebra

$$\begin{aligned} \gamma_k &= a_k + a_k^\dagger & \bar{\gamma}_k &= \frac{(a_k - a_k^\dagger)}{i} \\ a_k &= \frac{\gamma_k + i\bar{\gamma}_k}{2} & a_k^\dagger &= \frac{\gamma_k - i\bar{\gamma}_k}{2} \end{aligned}$$

to define the edge and vertex operators

$$E_{jk} := -i\gamma_j\gamma_k, \quad V_j := -i\gamma_j\bar{\gamma}_j$$

and then reconstructing the even fermionic operators

$$\begin{aligned} a_k^\dagger a_k &= \frac{(1 - V_k)}{2} & a_j^\dagger a_k &= \frac{i}{4}(1 - V_j)(1 + V_k)E_{jk} \\ a_j a_k &= \frac{i}{4}(1 + V_j)(1 + V_k)E_{jk} & a_j^\dagger a_k^\dagger &= \frac{i}{4}(1 - V_j)(1 - V_k)E_{jk} \end{aligned}$$

Let us consider how this looks for the simplified Fermi-Hubbard model on a square lattice with spin-spin interaction, which is given by the Hamiltonian

$$H = \sum_{(i,j),\sigma \in \{\uparrow,\downarrow\}} -t_{ij} \left(a_{i,\sigma}^\dagger a_{j,\sigma} + a_{j,\sigma}^\dagger a_{i,\sigma} \right) + U \sum_i a_{i\uparrow}^\dagger a_{i\uparrow} a_{i\downarrow}^\dagger a_{i\downarrow} \quad (5)$$

It is important to note that in the Fermi-Hubbard model there is no particle exchange between spin sectors. Therefore one does not need to encode edge operators between the modes in different spin sectors. For the sake of clarity we present the layout of encodings for one spin sector, which takes the form of a 2D planar graph. One may imagine performing an encoding on the other spin sector and layering it on top of the first, so that the spins on the same sites are near one another. This leads to a non-planar connectivity graph.

We can expand the hopping term into edge and vertex operators, temporarily dropping the uniform spin index.

$$a_i^\dagger a_j + a_j^\dagger a_i = \frac{-i}{2}(E_{ij}V_j + V_iE_{ij}) \quad (6)$$

And we can expand the spin-spin interaction

$$a_{i\uparrow}^\dagger a_{i\uparrow} a_{i\downarrow}^\dagger a_{i\downarrow} = \frac{1}{4}(1 - V_{i,\uparrow})(1 - V_{i,\downarrow}) \quad (7)$$

5 Square Lattice Encoding

Consider fermions living on a square lattice. We wish to encode these fermions onto qubits. For each vertex of the lattice, define a vertex qubit indexed by the fermionic site j . We now wish to label the faces of the lattice even and odd in a checker-board pattern. For the sake of clarity, let us assume to begin with that there are in total an even number of faces, and so an equal number of even and odd faces. We examine the case of an odd number of faces in Section 5.1. Note that the lattice may have unequal side lengths.

Associate a face qubit to the odd faces, as illustrated in Figure 1. Give an orientation to the edges of the lattice so that they circulate around the even faces clockwise or counterclockwise, alternating on every row of faces, also illustrated in Figure 1.

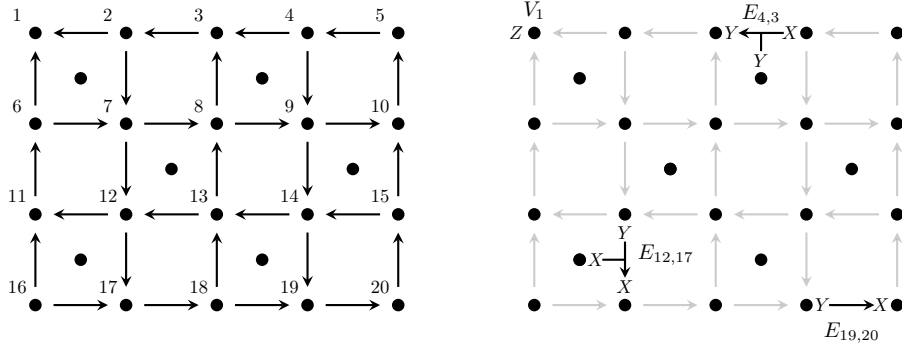


Figure 1: (Left) Edge orientation for the encoding on a 4×5 square lattice. (Right) Examples of encoded edge and vertex operators based on this layout.

Let $f(i, j)$ index the unique odd face adjacent to edge (i, j) . For every edge (i, j) , with i pointing to j , define the following encoded edge operators².

$$\tilde{E}_{ij} := \begin{cases} X_i Y_j X_{f(i,j)} & \text{if } (i, j) \text{ is oriented downwards} \\ -X_i Y_j X_{f(i,j)} & \text{if } (i, j) \text{ is oriented upwards} \\ X_i Y_j Y_{f(i,j)} & \text{if } (i, j) \text{ is horizontal} \end{cases} \quad (8)$$

$$\tilde{E}_{ji} := -\tilde{E}_{ij}. \quad (9)$$

For those edges on the boundary which are not adjacent to an odd face, we omit the third Pauli operator which is meant to be acting on the non-existent face qubit. For every vertex j define the encoded vertex operators

$$\tilde{V}_j := Z_j \quad (10)$$

This specifies all encoded vertex and edge operators. This encoding is illustrated in Figure 1.

It is not difficult to see that this encoding satisfies all of equations 1, 2 and 3. The intuition is that one may think of a directed edge as having an X on the tail and a Y on the head. Whenever the head of one edge touches the tail of another, then those two edge operators anti-commute, while if two edges touch head to head or tail to tail, then they commute. By adding a qubit at some faces, and choosing an appropriate orientation for the edges, one can enforce the additional necessary anti-commutation relations at the face qubits, as has been done here.

For M fermionic modes, this encoding uses fewer than $1.5M$ qubits. Most importantly this construction results in Fermi-Hubbard terms with Pauli weight at most 3. A critical feature which makes the Pauli weights and qubit numbers

²The difference in sign introduced between the vertical up and down arrows is merely to ensure that cycles around odd faces are equal to 1 and not -1 .

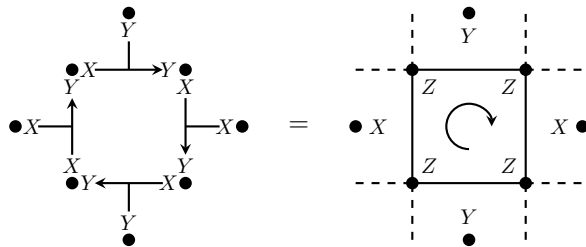


Figure 2: Non-trivial cycle stabilizer of the encoding. If a cycle is on the boundary of the lattice, omit any Pauli operators for which no face qubits exist.

so low is that the face qubits are used extremely efficiently, each one enforcing anti-commutation relations at four bounding corners.

Just as in the Bravyi-Kitaev superfast encoding, this encoding also demands that we restrict to a stabilizer code space, in order to satisfy Equation 4. The stabilizers \tilde{S}_p are indexed by all of the cycles p on the lattice, and are given by:

$$\tilde{S}_p = i^{(|p|-1)} \prod_{i=1}^{(|p|-1)} \tilde{E}_{p_i p_{i+1}}. \quad (11)$$

As in the superfast encoding, these stabilizers may be generated by the subset of cycles corresponding to cycles around faces. However unlike the superfast encoding, some of these stabilizers are equal to 1. Take for instance the cycle of edge operators going around vertices 4, 7, 8, 5 in Figure 1. The product of those edges is 1. This is true for every odd face. On the other hand the stabilizer cycles around even faces are non-trivial, and are illustrated in Figure 2. Therefore the number of independent stabilizer generators is half the number of faces, while the number of qubits is the number of fermionic modes plus half the number of faces. Thus the encoded Hilbert space is of the same dimension as the full fermionic Fock space. This is another major departure from the superfast encoding, which only encodes the even fermionic subspace.

Since the full fermionic Fock space is encoded, single fermions also admit a representation. It suffices to specify one Majorana operator, and all other fermions may be constructed using edge and vertex operators, and linear combinations of Majoranas. A logical Majorana operator γ_j must anti-commute with all edges adjacent to site j and the vertex operator V_j . Consider the corners of the lattice associated with an odd face. Such a corner j either has arrows pointing into it or pointing away from it. If the arrows point into the corner then choose the encoded Majorana operator to be $\tilde{\gamma}_j = X_j$, otherwise choose it to be $\tilde{\gamma}_j = Y_j$. The choice of corner is arbitrary. In the case of an even number of faces, there are two possible choices of corners, and once a corner is chosen, then the equivalent operator at the other corner corresponds to a Majorana hole operator $h_i := \gamma_i \prod_j V_j$.

5.1 Odd Number of Faces

If the lattice has an odd number of faces, then there are two possible checkerboard patterns. In one case (case (a)) there is an extra even face and every corner is even. In the other case (case (b)) there is an extra odd face and every corner is odd. Once a choice has been made, then one may proceed with constructing the encoding as prescribed in Section 5. This is illustrated in Figure 3.

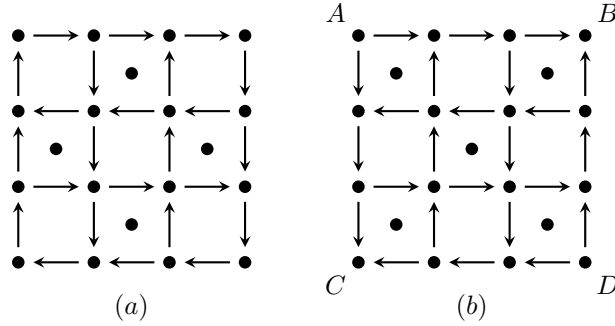


Figure 3: Two possible choices of encoding for a lattice with an odd number of faces.

In case (a) there is one more stabilizer than face qubit. Furthermore, it is not difficult to see that, up to stabilizers, $\prod_i \tilde{V}_i = 1$, and so in this case the code space is restricted to the even fermion subspace, just as in the superfast encoding. This is corroborated by the fact that, unlike for lattices with an even number of faces where a Majorana can be “injected” into an odd corner, here there are no odd corners in which to inject Majoranas, and so single fermion operators do not admit a representation in this code.

Case (b) is more interesting. Here there is one more face qubit than stabilizer, and so the encoded space is the full fermionic space plus one qubit degree of freedom: $\mathbb{C}^2 \otimes \mathbb{F}$. Furthermore there are four species of Majorana A_i , B_i , C_i and D_i , which may be injected at each of the four corners A , B , C , and D and then translated by edge operators to site i . These Majorana operators satisfy the following commutation and anti-commutation relations:

$$\{M_i, M_j\} = 0 \quad \forall M \in \{A, B, C, D\} \quad (12)$$

$$[M_i, M'_j] = 0 \quad \forall M \neq M' \in \{A, B, C, D\} \quad (13)$$

Furthermore these species of Majorana fuse into non-trivial string defects:

$$A \times B \approx C \times D \approx \epsilon_1 \quad (14)$$

$$A \times C \approx B \times D \approx \epsilon_2 \quad (15)$$

$$A \times B \times C \times D \approx 1 \quad (16)$$

Where this equivalence is modulo stabilizers and logical edge and vertex operations.

One may privilege one corner (let us choose A) as the Majorana operator on the fermionic system and the identity on the qubit system. The remaining corners may then be identified as hole operators on the fermionic system coupled to a Pauli operator on the qubit system

$$A_i = \mathbb{I} \otimes \gamma_i, \quad B_i = Y \otimes h_i, \quad C_i = X \otimes h_i, \quad D_i = Z \otimes h_i \quad (17)$$

recalling that $h_i = \gamma_i \prod_j V_j$. It then immediately follows that the non-trivial string defects correspond to Pauli operators on the logical qubit system.

$$\epsilon_1 \approx Y, \quad \epsilon_2 \approx X \quad (18)$$

The encoded \tilde{Y} and \tilde{X} operators are illustrated in Figure 4. They are strings of Z s along the bottom and right edge respectively, and strings of Y s along the bottom most row of faces and X s along the right most column of faces respectively. Note that if one treats one of these operators as a stabilizer, then one restricts to the full fermionic code space without an extra logical qubit. In this case, as one should expect, there are only two corners in which to inject a Majorana, since injecting a Majorana at either of the other two corners would anti-commute with the chosen stabilizer. These two species are clearly the Majorana and its hole counterpart.

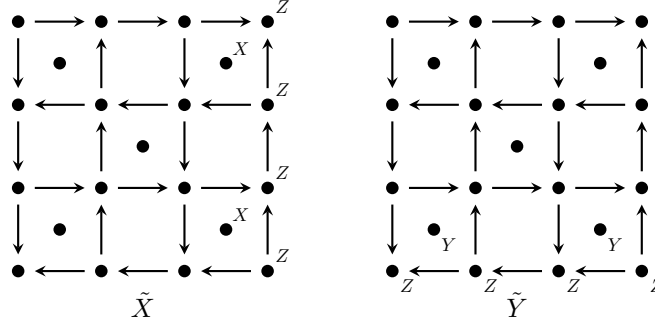


Figure 4: The logical X and Y operators on the extra logical qubit in case (b)

6 Hexagonal Lattice Encoding

Hexagonal lattices admit a similar construction to that outlined in Section 5. Again we follow the scheme of orienting the edges, introducing ansatz edge operators with an X at the tail and a Y at the head, and then introducing

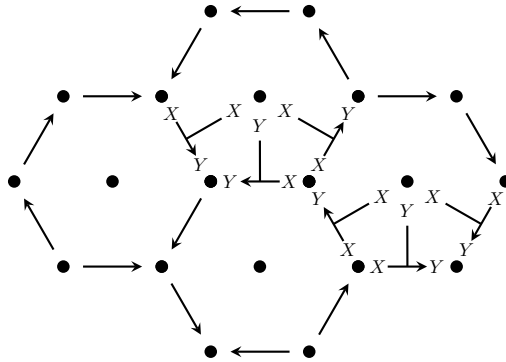


Figure 5: Edge orientation, qubit placement and edge operators for the hexagonal lattice encoding.

interactions on face qubits to satisfy the anti-commutation relations. Here we present the best construction we could find.

In the hexagonal lattice, we orient every edge except for the bottom edge of every face so that they circulate clockwise on even columns of faces and counterclockwise on odd columns, as illustrated in Figure 5. This ensures that heads touch tails for all edges except for the bottom edge of every hexagon. We also add a qubit at every face.

For every bottom edge of every face f , the edge operator acts on the face qubit of f with Y_f . The two edges adjacent to this bottom edge and also adjacent to f act on the face qubit of f with X_f . In this way all anti-commutation relations are satisfied. Just as in the square lattice case, the vertex operators are Z operators on the vertex qubit. We illustrate this construction in Figure 5.

Once again, the stabilizers of this encoding are cycles. However in this case there are no trivial cycles, so there is a stabilizer generator for every face. This implies that the code space is the full fermionic space. One again, single fermion operators may be injected into the code at those vertices from which edges are either uniformly pointing towards or away. Using this encoding for the Fermi-Hubbard model on a hexagonal lattice results in terms with Pauli weight at most 3. With M modes, this encoding uses fewer than $1.5M$ qubits.

7 Connection to the Toric Code

The observant reader will notice that on the square lattice one can make out the outline of the toric code. Indeed the stabilizers of the square lattice encoding are tensor products of toric code stabilizers on the face qubits (up to local rotations) and four qubit Z parity checks on the vertex qubits. This is illustrated in Figure 6. Here we present a way of formally understanding the significance of this synthesis.

An important feature of the toric code is that errors on the star and plaquette

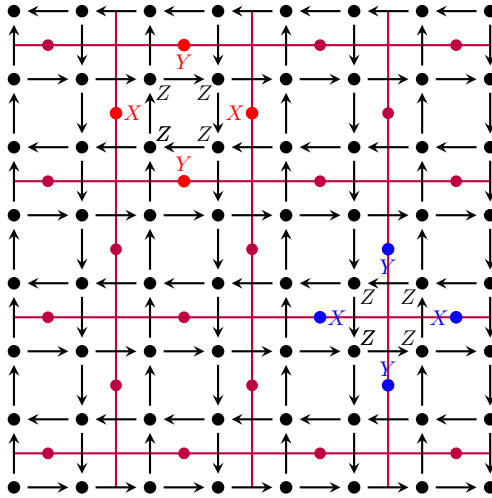


Figure 6: The toric code (purple) embedded in the square encoding. Each stabilizer of the square encoding is a tensor product of either a plaquette (red) or star (blue) operator, with a four qubit Z parity operator (black)

operators can be thought of as localised excitations, or particles. Conventionally these particles are labelled e and m for “electric” and “magnetic”. These particles exhibit non-trivial exchange statistics. e particles pick up a $+1$ phase when exchanged with other e particles, and similarly for m particles. But when e and m particles are exchanged, they pick up a global phase of -1 . Furthermore, e and m particles may be paired together and this pairing constitutes a third type of particle $\psi = e \times m$. This particle exhibits fermionic exchange statistics: when two ψ particles are exchanged they pick up a global phase of -1 . Furthermore, ψ particles are self annihilating, so they correspond to Majorana fermions.

Obviously the toric code does not encode these particles, since they do not commute with the stabilizers. However by coupling the toric code stabilizers to the stabilizers of another code, in this case the four qubit Z parity check operators, one can select out the ψ excitations and pull them into the code space. More concretely, consider that an edge operator $E_{ij} = -i\gamma_i\gamma_j$ corresponds to the creation of a pair of Majoranas at sites i and j . Similarly for any path between site i and site j composed of consecutive edge operators. Figure 7 illustrates an example of such a path of edge operators in the square encoding, and how this path gives rise to two ψ excitations in the toric code embedded in the encoding. It is not difficult to see that although the toric code stabilizers would normally raise an error under this circumstance, the Z parity check operators to which the toric code stabilizers are paired, also raise an error, and these errors cancel.

We believe the fundamental logic behind this synthesis is present in other local fermionic encodings. Indeed the toric code also appears in the hexagonal encoding presented here. The toric code is also recognisable in the Verstraete-

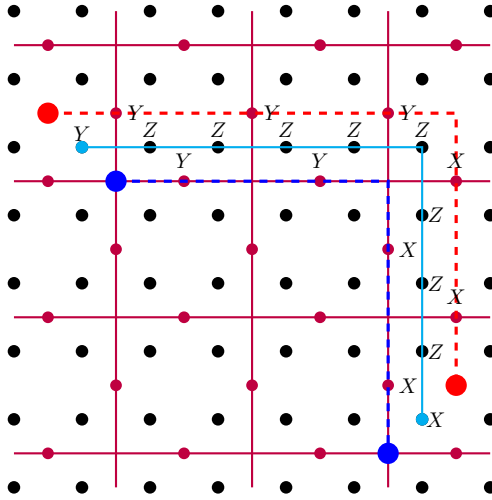


Figure 7: Majoranas (cyan), generated by a string of edge operators (cyan) in the square encoding correspond directly to pairs of e (blue) and m (red) particles in the toric code.

$$\begin{array}{c}
 \bullet \text{---} Y \text{---} \bullet \\
 | \\
 Y \quad X \\
 | \\
 \bullet \text{---} X \text{---} \circ \text{---} Z \text{---} \\
 | \\
 Z \\
 |
 \end{array}
 =
 \begin{array}{c}
 \bullet \text{---} Y \text{---} \bullet \\
 | \\
 Y \quad Y \\
 | \\
 \bullet \text{---} Y \text{---} \circ \\
 | \\
 Z \\
 |
 \end{array}
 \times
 \begin{array}{c}
 | \\
 Z \\
 | \\
 \circ \text{---} Z \text{---} \\
 | \\
 Z \\
 |
 \end{array}$$

Figure 8: How a cycle stabilizer from the BKSF encoding splits into a plaquette and star operator from the toric code, the vertex at which they overlap is highlighted. This is the case if the incidences are ordered {north, east, south, west}, any clockwise or counter-clockwise ordering will result in a similar stabilizer which may have a different orientation.

Circ encoding. Additionally the cycle stabilizers of the Bravyi-Kitaev Superfast (BKSF) encoding correspond to products of adjacent star and plaquette operators of the toric code³ (see Figure 8), so that the BKSF encoding can be thought of as the stabilizer code generated by a particular choice of subgroup of the stabilizer group of the toric code, such that ψ particles do not flag as errors. This last example most cleanly illustrates what we believe is the underlying mechanism at play in all of these encodings: it is the topological order of the toric code which gives rise to the fermionic non-locality.

³This is true for particular choices of incidence orderings when defining the code (see [BK02]). If other orderings are chosen then the encoding relates to a toric-like code in which the plaquette operators take a different form. Furthermore, the encoding presented in [Jia+18] can also be related to a modified toric code with different plaquette *and* star operators which vary across the lattice.

8 Discussion

The fermion to qubit encodings presented here constitute a significant improvement on both the mode to qubit ratio and the Pauli weights of local operators. Although we have emphasized how these encodings give rise to low weight terms in the Fermi-Hubbard model, any fermionic Hamiltonian which is local on these graphs and whose terms are products of small numbers of vertex and edge operators will also be of similarly low weight. These encodings are tailored to the square and hexagonal lattices, however we strongly expect a generalisation can be devised for some larger families of graphs, for example some subset of planar graphs with vertex degree no more than four. Indeed we have found a number of other planar graphs which yield to this construction. Furthermore, this construction can be generalised to higher dimensions, in particular to 3d cubic lattices [DK20].

We conjecture that no fermion to qubit encodings exist which have a smaller upper bound on the Pauli weights of vertex and edge operators.

Since this fermionic encoding has low weight edge and vertex operators, it is necessarily a low distance code. For example a Z error on any vertex qubit corresponds to a logical vertex operation. In concurrent work [Bau+20] we argue that for certain purposes this may not pose as serious a problem as one might expect.

From the perspective of implementations one downside to these encodings is that it is not clear that the low weight property can be preserved when restricting to hardware with a planar interaction graph and including all spins. This is not something widely considered in most other works, besides [SW19], and so it may be that this encoding still performs comparatively well under this restriction.

Ref. [CBC20] proposes a novel pulse based scheme for simulating time evolution of quantum systems. One of the primary bottlenecks for the performance of this scheme is the Pauli weight of the encoded Hamiltonian terms. By employing the encoding in this work, simulations using such a pulse based scheme are expected to see an order of magnitude improvement in performance over Verstraete-Cirac, which has max weight 4 terms.

9 Acknowledgements

We would like to thank Johannes Bausch, Toby Cubitt, and Laura Clinton for their helpful discussions with us, and Johannes Bausch and Toby Cubitt for their thorough proofreading.

References

- [WJ28] Eugene P Wigner and Pascual Jordan. “Über das Paulische Äquivalenzverbot”. *Z. Phys* 47 (1928), p. 631.

- [BK02] Sergey B Bravyi and Alexei Yu Kitaev. “Fermionic quantum computation”. *Annals of Physics* 298.1 (2002), pp. 210–226.
- [LW03] Michael Levin and Xiao-Gang Wen. “Fermions, strings, and gauge fields in lattice spin models”. *Phys. Rev. B* 67 (24 2003), p. 245316.
- [VC05] Frank Verstraete and J Ignacio Cirac. “Mapping local Hamiltonians of fermions to local Hamiltonians”. *Journal of Statistical Mechanics: Theory and Experiment* 2005.09 (2005), P09012.
- [WHT16] James D. Whitfield, Vojtěch Havlíček, and Matthias Troyer. “Local spin operators for fermion simulation”. *Phys. Rev. A* 94 (3 Sept. 2016), p. 030301.
- [Jia+18] Zhang Jiang, Jarrod McClean, Ryan Babbush, and Hartmut Neven. “Majorana loop stabilizer codes for error correction of fermionic quantum simulations”. *arXiv preprint arXiv:1812.08190* (2018).
- [SW19] Mark Steudtner and Stephanie Wehner. “Quantum codes for quantum simulation of fermions on a quantum processor”. *Phys. Rev. A* 99 (2 2019), p. 022308.
- [Set+19] Kanav Setia, Sergey Bravyi, Antonio Mezzacapo, and James D Whitfield. “Superfast encodings for fermionic quantum simulation”. *Physical Review Research* 1.3 (2019), p. 033033.
- [HTW17] Vojtěch Havlíček, Matthias Troyer, and James D. Whitfield. “Operator locality in the quantum simulation of fermions”. *Phys. Rev. A* 95 (3 2017), p. 032332.
- [Cad+19] Chris Cade, Lana Mineh, Ashley Montanaro, and Stasja Stanisic. *Strategies for solving the Fermi-Hubbard model on near-term quantum computers*. 2019. arXiv: 1912.06007 [quant-ph].
- [DK20] Charles Derby and Joel Klassen. *in preparation*. 2020.
- [Bau+20] Johannes Bausch, Toby S. Cubitt, Charles Derby, and Joel Klassen. “Mitigating Errors in Local Fermionic Encodings”. 2020.
- [CBC20] Laura Clinton, Johannes Bausch, and Toby S. Cubitt. “Hamiltonian Simulation Algorithms for Near-Term Quantum Hardware”. 2020.
- [Ott95] Johnny T. Ottesen. *Infinite Dimensional Groups and Algebras in Quantum Physics*. Berlin, Heidelberg: Springer Berlin Heidelberg, 1995, pp. 13–59.

A Proof of Correctness of Fermionic Encodings

For the sake of completeness we include here a more explicit proof of our claims. The arguments presented here should be relatively familiar to those readers acquainted with fermionic encodings.

Definition 1. *An encoding from some Hilbert space H_1 to another Hilbert space H_2 is an isometry ⁴ $J : H_1 \rightarrow H_2$, as defined in [BK02, Sec. 5].*

Let $f_m = \mathbb{C}^m$ correspond to an m mode single fermion Hilbert space. The n fermion Fock space on m modes is defined as

$$\wedge^n f_m = \text{span} \left(\frac{1}{n!} \sum_{\pi \in S_n} \text{sgn}(\pi) \bigotimes_{i=1}^n \psi_{\pi(i)} : \psi_j \in f_m \right),$$

and the full fermionic Fock space of m modes is $F_m = \bigoplus_{n=0}^m (\wedge^n f_m)$. The dimension of F_m is 2^m . Let $F_m^E = \bigoplus_{n \in \text{even}} (\wedge^n f_m)$ and $F_m^O = \bigoplus_{n \in \text{odd}} (\wedge^n f_m)$. If m is even the dimension of F_m^E is 2^{m-1} .

In the following we denote with $L(S)$ to be the Linear operators on a space S , which form a C^* -algebra in the case where S is a complex Hilbert space.

Definition 2 (Fermionic Encoding). *A fermionic encoding is an isometry $J : F_m \rightarrow H$, where H is a qubit Hilbert space, i.e. J satisfies the property $J^\dagger J = \mathbb{I}_{F_m}$*

Proposition 1 ([BK02]). *A $*$ -isomorphism $\mu : L(H_1) \rightarrow L(H_2)$ induces an encoding $J : H_1 \rightarrow H_2$ which is unique up to a global phase. An operator $X \in L(H_1)$ is represented via the map $\mu(X) = JXJ^\dagger$.*

Proposition 2 ([BK02]). *The algebra $L(F_m^E) \oplus L(F_m^O)$ is generated by the edge and vertex operators E_{ij} and V_i . The algebra $L(F_m)$ is generated by a single Majorana operator γ and the edge and vertex operators E_{ik} and V_i .*

Theorem 1. *A square lattice encoding with an even number $(L_1 \times L_2)$ of faces given in Section 5 describes an encoding $J : F_m \rightarrow \mathcal{L}$, where $m = (L_1 + 1)(L_2 + 1)$ and $\mathcal{L} \subset (\mathbb{C}^2)^{m + L_1 L_2 / 2}$.*

Proof. The encoding employs $m + L_1 L_2 / 2$ qubits. The number of non-trivial stabilizers is $L_1 L_2 / 2$. Let $\mathcal{L} \subset H = (\mathbb{C}^2)^{m + L_1 L_2 / 2}$ be the joint $+1$ eigenspace of these non-trivial stabilizers, then $\dim(\mathcal{L}) = 2^m = \dim(F_m)$.

If edge operators E_{jk} and vertex operators V_k satisfy the relations given in eqs. (1) to (4), they generate the even fermionic algebra $L(F_m^E)$. In order to generate the entire fermionic algebra $L(F_m)$, we need an additional generator; for instance a single Majorana operator γ_i , which together with a vertex operator $V_i \gamma_i \propto \tilde{\gamma}_i$ generates the entire algebra $L(F_m)$.

By inspection the Pauli operators \tilde{E}_{jk} and \tilde{V}_k satisfy the relations given in eqs. (1) to (3). Furthermore, since the number of faces is even there are always

⁴ $J^\dagger J = \mathbb{I}_{H_1}$ and $JJ^\dagger = \text{Proj}(\text{Image}(J))$

exactly two corner faces of the lattice which are odd according to the checker-board labelling. Choose a corner vertex c , associated with an odd corner face, and define an encoded Majorana operator

$$\tilde{\gamma}_c = \begin{cases} X_c & \text{arrows pointing into corner, or} \\ Y_c & \text{otherwise.} \end{cases}$$

Then $\{\tilde{\gamma}_c, \tilde{E}_{jk}\} = \{\tilde{\gamma}_c, \tilde{V}_k\} = 0$.

By inspection we see that \tilde{E}_{jk} , \tilde{V}_k and the additional Majorana $\tilde{\gamma}_c$ commute with the stabilizers given in eq. (11); as such, restriction to the joint $+1$ eigenspace \mathcal{L} of the stabilizers—denoted $\cdot|_{\mathcal{L}}$ —retains all their algebraic properties. Furthermore, the operators $\tilde{E}_{jk}|_{\mathcal{L}}$ satisfy eq. (4). Thus by the same argument as in [BK02, Sec. 8], the identification

$$E_{jk} \mapsto \tilde{E}_{jk}|_{\mathcal{L}} \quad V_k \mapsto \tilde{V}_k|_{\mathcal{L}} \quad \gamma_c \mapsto \tilde{\gamma}_c|_{\mathcal{L}}$$

extends to a $*$ -homomorphism $\mu : L(F_m) \rightarrow L(\mathcal{L})$. Since the CAR algebra is unique up to an isomorphism [Ott95], and $\dim(\mathcal{L}) = \dim(F_m)$, the mapping is an isomorphism. The claim follows by proposition 1. \square

Theorem 2. *A square lattice encoding with an odd number $(L_1 \times L_2)$ of faces, and an extra even face (case a), as given in Section 5.1, describes an encoding $J : F_m^E \rightarrow \mathcal{L}$, where $m = (L_1 + 1)(L_2 + 1)$ and $\mathcal{L} \subset (\mathbb{C}^2)^{m + \lfloor L_1 L_2 / 2 \rfloor}$.*

Proof. The encoding employs $m + \lfloor L_1 L_2 / 2 \rfloor$ qubits. The number of non-trivial stabilizers is $\lfloor L_1 L_2 / 2 \rfloor$. Let $\mathcal{L} \subset (\mathbb{C}^2)^{m + \lfloor L_1 L_2 / 2 \rfloor}$ be the $+1$ eigenspace of the non-trivial stabilizers, then $\dim(\mathcal{L}) = 2^{m + \lfloor L_1 L_2 / 2 \rfloor - \lfloor L_1 L_2 / 2 \rfloor} = 2^{(m-1)}$. Since $L_1 L_2$ is odd, it must be the case that L_1 and L_2 are odd, and so m is even. Thus $\dim(F_m^E) = 2^{m-1} = \dim(\mathcal{L})$.

$L(F_m^E) \oplus L(F_m^O)$ is generated by E_{ij} and V_i . However under the algebraic constraint that $\prod_i V_i = \mathbb{I}$, the algebra only generates $L(F_m^E)$. Thus we have a mapping $\mu : L(F_m^E) \rightarrow L(\mathcal{L})$ by $\mu(E_{ij}) = \tilde{E}_{ij}|_{\mathcal{L}}$ and $\mu(V_i) = \tilde{V}_i|_{\mathcal{L}}$. By a similar argument to the previous theorem, μ is a $*$ -isomorphism, and therefore specifies an encoding $J : F_m^E \rightarrow \mathcal{L}$. \square

Theorem 3. *A square lattice encoding with an odd number $(L_1 \times L_2)$ of faces, and an extra odd face (case b), as given in Section 5.1, describes an encoding $J : \mathbb{C}^2 \otimes F_m \rightarrow \mathcal{L}$, where $m = (L_1 + 1)(L_2 + 1)$ and $\mathcal{L} \subset (\mathbb{C}^2)^{m + \lfloor L_1 L_2 / 2 \rfloor}$.*

Proof. The encoding employs $m + \lfloor L_1 L_2 / 2 \rfloor$ qubits. The number of non-trivial stabilizers is $\lfloor L_1 L_2 / 2 \rfloor$. Let $\mathcal{L} \subset (\mathbb{C}^2)^{m + \lfloor L_1 L_2 / 2 \rfloor}$ be the $+1$ eigenspace of the non-trivial stabilizers, then $\dim(\mathcal{L}) = 2^{(m+1)} = \dim(\mathbb{C}^2 \otimes F_m^E)$.

There are four corner faces of the lattice which are odd according to the checker-board labelling. One may choose a corner vertex c and define an encoded operator acting trivially on the logical qubit, and as a Majorana on the logical fermionic space: $\tilde{\mathbb{I}} \otimes \tilde{\gamma}_c = X_c$ or Y_c depending on if the arrows point into or respectively away from that corner. The other three corners, which we label

c_x, c_y, c_z , may then be defined as logical Pauli operators combined with logical hole operators:

$$\begin{aligned}\tilde{X} \otimes \tilde{h}_{c_x} &= X_{c_x} \text{ or } Y_{c_x} \\ \tilde{Y} \otimes \tilde{h}_{c_y} &= X_{c_y} \text{ or } Y_{c_y} \\ \tilde{Z} \otimes \tilde{h}_{c_z} &= X_{c_z} \text{ or } Y_{c_z}\end{aligned}$$

here the choice of which corners to associate with which logical Paulis is a matter of convention, and the choice of X or Y will again depend on if the arrows point into or respectively away from that corner.

By Proposition 2, the operators $\mathbb{I} \otimes \gamma_j$, $X \otimes h_j$ and $Y \otimes h_j$, along with the edge and vertex operators, generate $L(\mathbb{C}^2 \otimes F_m)$. Define the mapping $\mu : L(\mathbb{C}^2 \otimes F_m) \rightarrow L(\mathcal{L})$ by $\mu(\mathbb{I} \otimes \gamma_c) = \tilde{I} \otimes \tilde{\gamma}_c|_{\mathcal{L}}$ etc. By a similar argument to the previous theorems, μ is a *-isomorphism, and therefore specifies an encoding $J : \mathbb{C}^2 \otimes F_m \rightarrow \mathcal{L}$.

□